RSC Advances

ROYAL SOCIETY OF CHEMISTRY

www.rsc.org/advances

RSC Advances

ARTICLE

Novel Conductive Core-shell Particles of Elastomeric Nanoparticles Coated with Polypyrrole

Received 00th January 20xx,
Accepted 00th January 20xx

DOI: 10.1039/x0xx00000x

www.rsc.org/

Jiangru Zhang, [a] Guicun Qi, [a] Xiang Wang, [a] Binghai Li, [a] Zhihai Song, [a] Yue Ru, [a] Xiaohong Zhang[a]* and Jinliang Qiao[a]*

For the first time, an ultrafine conductive particle with core-shell structure, acrylonitrile-butadiene elastomeric nanoparticle (NBR-ENP) coated with polypyrrole (PPy), was prepared by in-situ oxidative polymerization. The resistivity of NBR-ENP/PPy particle could reach to 25 Ω·m. By using NBR-ENP/PPy latex, PVA/NBR-ENP/PPy composite with resistivity of 170 Ω·m was prepared. For comparison, carboxylic acrylonitrile butadiene-ENP/polypyrrole (CNBR-ENP/PPy) with core-shell structure and styrene butadiene-ENP/polypyrrole (SBR-ENP/PPy) with raspberry-like structure were also prepared. It was found that both CNBR-ENP/PPy and SBR-ENP/PPy have much higher resistivity compared with NBR-ENP/PPy. Their resistivity differences were analyzed and the possible reason was proposed.

1. Introduction

Inherently conducting polymers (ICPs) have been an area of intense interest over the past 40 years. The Nobel Prize in Chemistry 2000 was awarded jointly to Alan J. Heeger, Alan G. MacDiarmid and Hideki Shirakawa for "the discovery and development of conductive polymers". The unique feature of ICPs is that they combine the properties of two widely divergent classes of materials: plastics and metals.[1] However, the industrial applications of ICPs are limited because some of its disadvantages. Polyacetylene has good mechanical properties and very high conductivity in a doped state, but very poor stability at ambient conditions.[2] Polypyrrole (PPy), polyaniline (PANI), polythiophene (PTh) and other ICPs prepared from heterocyclic monomers exhibit high conductivity and stability.[3] They, however, are intractable materials, namely insoluble and infusible owing to their high crystallinity, crosslinking and backbone rigidity.[4] Many attempts have been made to improve the poor processability of ICPs, such as introducing bulky side groups,[5] synthesizing nanoparticles[6-8] and forming blend or composites with other polymers.[4, 9-11] Coating ICPs onto polymer latex particle is also an important method to improve the processibility of ICPs. Yassar et al.[12] coated PPy onto the submicronic polystyrene (PS) latex particles derivatized either with sulphonic or carboxylic groups.[13, 14] Lu Y et al.[15] coated PPy onto the surface of polystyrene-poly(ethylene glycol) monomethacrylate (PS-PEGMA) latex particles with diameter of 120 to 300 nm. The research group at DSM has shown that commercial aqueous resin dispersions, stabilized by non-ionic surfactants, can be coated with PPy or PANI.[16] Armes et al. have done lots of work with respect to coating ICPs onto the surface of micrometer-sized PS,[11, 17-23] poly(methyl methacrylate) (PMMA),[24] poly(n-butyl methacrylate) (PBMA)[25] and poly[bis(4-vinylthiophenyl)sulfide] (PMPV).[26, 27] When coating PPy onto the submicrometer-sized poly(ethylene glycol)-stabilized PS latex particles, Cairns et al. [28] found that the PPy could deposit onto the latex particles as discrete PPy nanoparticles with diameter of 20-30 nm. These nanoparticles may act as bridging flocculants or binders, leading to hetero-flocculation of the PS latex.[28, 29] Wu Q et al.[30, 31] coated PANI onto PS emulsifier-free latex particles by a diffusion-interface-polymerization process. The deposited PANI layer was more uniform than conventional method. It is also found that the PPy layer deposited on PS latex particles was smoother and more uniform when the latex was stabilized by anionic emulsifier than by hydrophilic groups.[32] Moreover, Bai M Y et al.[33]also obtained smooth and uniform PPy and PANI coating on commercial PS beads pre-treated with concentrated sulfuric acid. Besides, silica submicrospheres have also been coated by PPy[34] or PEDOT[35] layer. In summary, it can be found that almost all these polymers coated by ICPs are rigid. And elastomeric nanoparticles (ENPs) have never been coated by ICPs. The advantages of coating ICPs on soft ENP instead of rigid polymer are that soft ENP/ICP particles can be very easy to disperse well in polymer matrix. Similar to inorganic nano-particle, rigid polymer/ICP particles, however, are extremely difficult to disperse in polymer matrix. Therefore, better conductivity is expected when soft ENP/ICP particles are used to modify polymers. It is well known that the preparation of soft ENPs/ICPs particles is much more difficult than that of rigid polymer/ICPs particles.

In our previous studies, a series of ENPs have been developed by a novel process.[36-45] The typical feature of ENPs is that they can be stretched and deformed under shear force

[a] SINOPEC Beijing Research Institute of Chemical Industry, Beijing 10013.
* Corresponding author: Jinliang Qiao (qiaojl.bjhy@sinopec.com)
Xiaohong Zhang (zhangxh.bjhy@sinopec.com).

and can be recovered after the force is taken off. Therefore, the ENPs have excellent dispersability in various matrixes, especially in plastic matrix.[46, 47] Furthermore, the ENPs can also promote the dispersion of other fillers.[48-56] In this work, we try to use ENPs to develop a novel strategy to improve the processibility of PPy. We hope this new strategy can have impact in the manufacture of composites materials with controlled electrical resistivity and processability.

2. Experimental

2.1 Materials

Pyrrole monomer was purchased from Aladdin Industrial Corporation. Polyvinylpyrrolidone (PVP) (K-30, Mw: 10,000-70,000) was purchased from Xilong Chemical Co., Ltd. Polyvinyl alcohol (PVA, CP-1000) was purchased from Kuraray. Toluene-4-sulfonic acid monohydrate (p-TSA), 30 wt% hydrogen peroxide (H_2O_2) and iron (III) chloride hexahydrate ($FeCl_3 \cdot 6H_2O$) were all purchased from Sinopharm Chemical Reagent. Acrylonitrile-butadiene rubber (NBR) latex (solid content 45 wt%, acrylonitrile content 26 wt%, supplied by Tianyuan Chemical Co. in Zhaodong, Heilongjiang province), carboxylic acrylonitrile-butadiene rubber (CNBR) latex (solid content 45 wt%, acrylonitrile content 26 wt%, carboxylic content 2 wt%) supplied by Tianyuan Chemical Co. in Zhaodong, Heilongjiang province and styrene-butadiene rubber (SBR) latex (solid content 45 wt%, weight ratio of styrene/butadiene is 1) supplied by Zibo Xiangda Chemcial Co. LTD were used directly without any further purification.

2.2 Preparation of ENP/PPy Latex

2.2.1 Preparation of NBR-ENP/PPy latex. The NBR latex was crosslinked by Co^{60} radiation with adsorption dose of 25 KGy and dose rate of 50 Gy/min first, and then the crosslinked NBR-ENP latex (30 g) was introduced into three-necked round-bottomed flask. Pyrrole monomer (1.4 g) was dropped slowly into stirred reaction solution and swelled for 1h. Then 50 ml PVP aqueous solution (0.36 M for NBR-ENP/PPy-I, 0.18 M for NBR-PPy-II) was added into the flask. And p-TSA (80 ml, 0.12 M) and $FeCl_3 \cdot 6H_2O$ (20 ml, 1.85 mM) aqueous solutions were dropped successively into the flask slowly. The reaction flask was cooled in ice-water bath. Finally, the 30 wt% H_2O_2 solution (2.8 g) diluted by de-ionized water was introduced into the flask. The polymerization was carried out at 0-5 °C for 48 h.

2.2.2 Preparation of CNBR-ENP/PPy latex. The CNBR latex was crosslinked by Co^{60} radiation with adsorption dose of 25 KGy and dose rate of 50 Gy/min first to prepare CNBR-ENP latex. Then the preparation process of CNBR-ENP/PPy latex was similar with NBR-ENP/PPy except that CNBR-ENP latex (30 g) was used instead of NBR-ENP latex and the concentration of stabilizer PVP was 0.18 M. Other conditions are the same with those used in part 2.2.1.

2.2.3 Preparation of SBR-ENP/PPy latex. Firstly, the SBR latex was crosslinked by Co^{60} radiation with adsorption dose of 25 KGy and dose rate of 50 Gy/min to prepare SBR-ENP latex. And SBR-ENP latex (40 g) was introduced into three-necked round-bottom flask. Secondly, PVP (55 ml, 0.56 M), p-TSA (10 ml, 2.68 M), $FeCl_3 \cdot 6H_2O$ (10 ml, 0.004 M) and H_2O_2 (12.6 ml, 5.32 M) aqueous solutions were sequently added to SBR-ENP latex. Finally, pyrrole aqueous solution (200 ml, 0.34 M) was dropped into flask during 4 h. The reaction was carried out at 10-15 °C for 48 h.

The obtained NBR-ENP/PPy, CNBR-ENP/PPy and SBR/PPy latex were filtered and almost no precipitation was found, suggesting that the emulsions were stable during the reaction. The shelf stabilities of these emulsions were over six months. The obtained emulsions were stable because the amount of compound oxidant $FeCl_3 \cdot 6H_2O$ was very little, the adding rates of pyrrole and other solutions were very slow, and the macromolecular stabilizer PVP also helped improve the latex stability.

2.2.4 Preparation of PVA/NBR-ENP/PPy-II composite. PVA/NBR-ENP/PPy-II composite was prepared by drying the mixture of 20 wt% PVA aqueous solution and NBR-ENP/PPy-II emulsion.

2.3 Characterization

Transmission electron microscope (TEM) characterizations were carried out on a FEI Tecnai 20 instrument operated at an acceleration voltage of 200 kV. A Reichert-Jung Ultracut-E microtome was utilized to prepare ultrathin sections of about 50-100 nm in thickness at -50 °C. The ultrathin sections were stained with osmium tetroxide (OsO_4) before TEM imaging. The surface morphologies of the samples were observed on a field-emission scanning electron microscopy (FE-SEM, S-4800, Hitachi, Japan) operated at 1 kV. Dynamic light scattering (DLS) measurements were carried out on a Malvern Nano-ZS device equipped with a He-Ne solid-state laser operating at 633 nm at 25 °C. Fourier transform infrared (FTIR) spectra were taken on a Nicolet Nexus 470 instrument. Thermogravimetric analysis (TGA) was obtained on STA 449 C Jupiter (Netzsch, Germany). The resistivities were measured on wafers obtained by drying the latexes using the RTS-8 type four-point probe conductivity meter (Guangzhou four-point probe technology Co., LTD, China) at room temperature.

3. Results and discussion

3.1 Characterization of NBR-ENP/PPy latex particles

Fig.1 are the TEM pictures of NBR-ENP (Fig. 1a and b), NBR-ENP/PPy-I (Fig. 1c and d) and NBR-ENP/PPy-II (Fig. 1e and f) particles, respectively. The amount of stabilizer PVP for NBR-ENP/PPy-II is lower than that for NBR-ENP/PPy-I. It can be found from Fig. 1a and b that the edges of NBR-ENP particles are ambiguous. Moreover, the contrast of NBR-ENP/PPy is distinctly sharper (Fig. 1c and e) than that of NBR-ENP (Fig. 1b). It can be found from Fig. 1d and f that the boundary of NBR-ENP/PPy particles is clear and the surface morphologies are rough compared with NBR-ENP particles. Therefore, it is clear that PPy has been deposited onto the surface of NBR-ENP latex particles successfully. Both NBR-ENP/PPy-I and NBR-ENP/PPy-II latex are stable. The resistivities for NBR-ENP/PPy-I and NBR-ENP/PPy-II measured by four-point probe conductivity meter

are 210 Ω·m and 25 Ω·m, respectively. It is obvious that the resistivity of NBR-ENP/PPy decreases as the amount of stabilizer decreases. The average diameter of NBR-ENP/PPy particles measured from TEM pictures is ca. 100 nm.

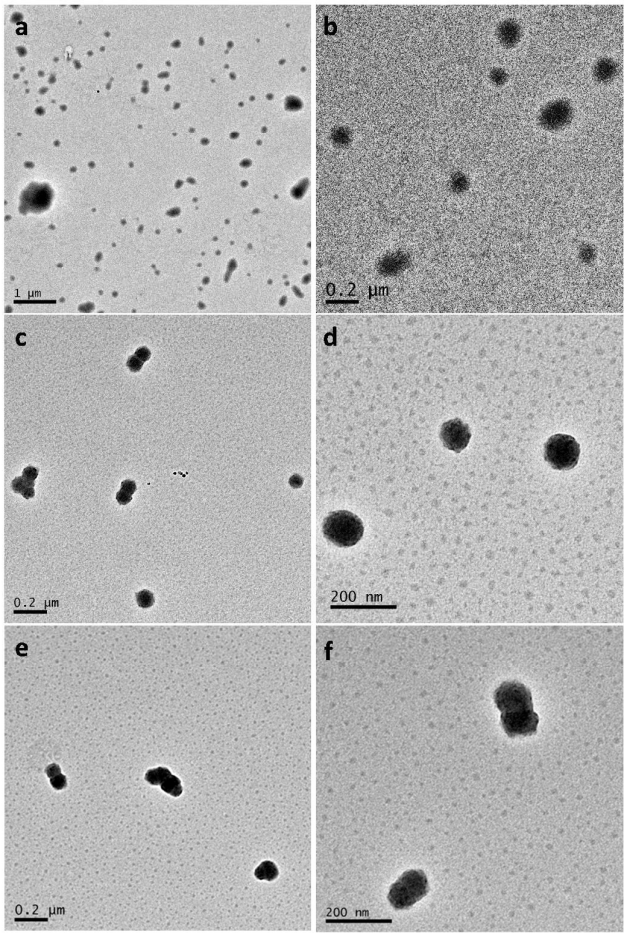

Fig. 1 The TEM pictures of NBR-ENP (a, b), NBR-ENP/PPy-I (c, d) and NBR-ENP/PPy-II (e, f) particles

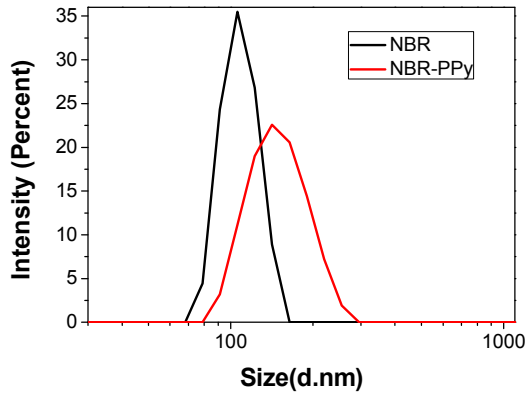

Fig.2 The Z-average diameter distributions for NBR-ENP and NBR-ENP/PPy-II latex particles

The Z-average diameter distributions of NBR-ENP and NBR-ENP/PPy latex particles measured by DLS are shown in Fig. 2. The Z-average diameters of NBR-ENP and NBR-ENP/PPy-II latex particles are about 100 nm and 150 nm, which confirm that PPy has been coated onto the surface of NBR-ENP latex particles.

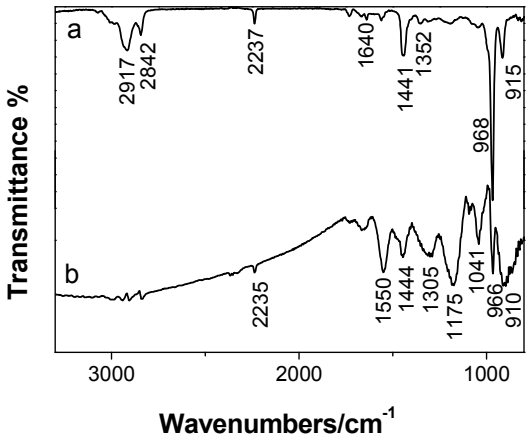

Fig. 3 The FTIR spectra of (a) NBR-ENP and (b) NBR-ENP/PPy-II particles

The FTIR spectra of NBR-ENP and NBR-ENP/PPy-II particles are shown in Fig. 3. In Fig. 3a, the characteristic absorptions of NBR-ENP particles are observed at 2917 cm^{-1} (asymmetric stretching vibration of $-CH_2-$), 2842 cm^{-1} (symmetric stretching vibration of $-CH_2-$), 2237 cm^{-1} (stretching vibration of $-C\equiv N$), 1640 cm^{-1} (stretch vibration of C=C), 1441 cm^{-1} (out of plane wagging vibration of $-CH_2-$) and 968 cm^{-1} (deformation vibration of C-H for trans $-CH_2CH=CHCH_2-$). In addition, the baseline in Fig. 3a is very flat. In contrast, in Fig. 3b, there is a broad absorption above 1600 cm^{-1}, arising from the free charge carriers present in the doped PPy. Furthermore, Fig. 3b contains several strong bands at 1550 cm^{-1} (C=C stretching vibration of the pyrrole ring), 1305 cm^{-1} (=CH- in plane vibration of the PPy), 1175 cm^{-1} (vibration of the aromatic pyrrole ring), 1041 cm^{-1} (C-H in-plane deformation vibration) and 910 cm^{-1} (N-H in-plane deformation vibration) due to the doped PPy component, while the intensities of the characteristic peaks of NBR-ENP are obviously attenuated, which confirm again that PPy has been deposited on NBR-ENP latex particles. Moreover, those characteristic peaks of NBR-ENP do not disappear totally in Fig. 3b. Therefore, the PPy coating should be not continuous or compact.

Thermogravimetric curves recorded in nitrogen for NBR-ENP and NBR-ENP /PPy-II particles are shown in Fig. 4. It can be found that the temperatures of maximum weight loss rate for NBR-ENP and NBR-ENP/PPy-II are almost the same, while the onset temperature of weight loss for NBR-ENP/PPy-II is much lower than that of NBR-ENP, which should be caused by the dehydration below 150 °C and the volatilization of the dopant p-toluene sulfonic acid at ca. 150-350 °C. The residue weights of NBR-ENP and NBR-ENP/PPy-II are respectively 4.87%

and 17.38%, therefore, it is inferred that PPy has been carbonized in nitrogen.

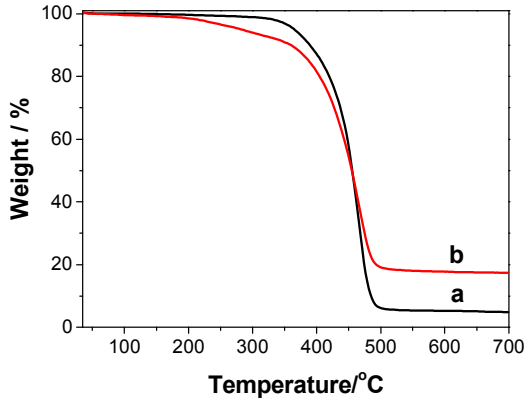

Fig. 4 TGA curves obtained in nitrogen for NBR-ENP (a) and NBR-ENP/PPy-II (b) particles

The TEM images of PVA/NBR-ENP/PPy-II composite stained with OsO_4 are shown in Fig. 5. The weight ratio of PVA and NBR-ENP/PPy-II is 3/7. PVA can't be stained by OsO_4 because it is saturated polymer. In contrast, NBR-ENP/PPy-II can be stained by OsO_4 as both NBR-ENP and PPy have unsaturated bonds. Thus, those black nanoparticles observed in Fig. 5 are NBR-ENP/PPy-II nanoparticles, whereas the part around NBR-ENP/PPy-II nanoparticles with white colour is PVA. The boundaries of NBR/PPy-II nanoparticles can be observed clearly, indicating that the dispersion of those NBR-ENP/PPy-II nanoparticles is excellent. The resistivity of the PVA/NBR-ENP/PPy-II composite measured by four-point probe conductivity meter is 170 Ω·m.

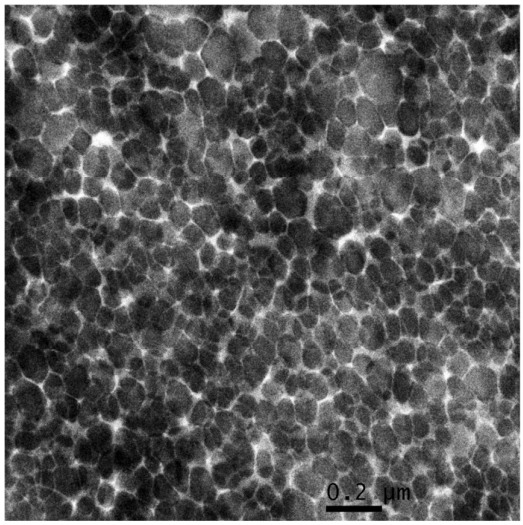

Fig. 5 The TEM image of PVA/NBR-ENP/PPy-II composite

3.2 Characterization of CNBR-ENP/PPy latex particles

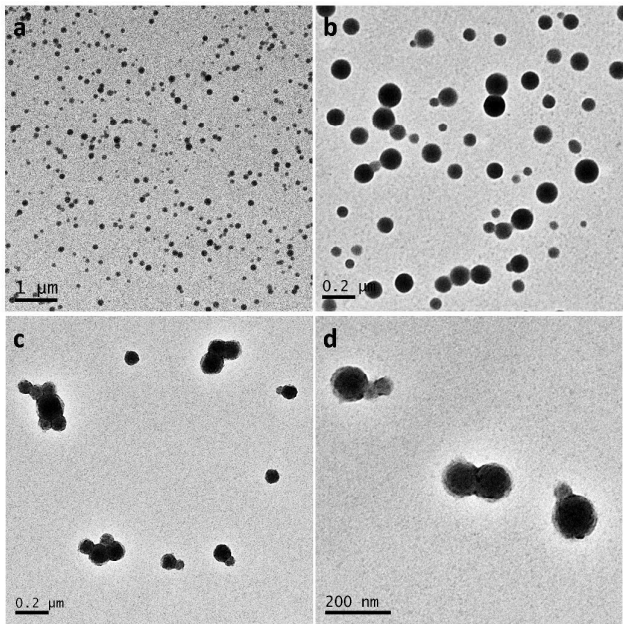

Fig. 6 The TEM pictures of CNBR-ENP (a, b) and CNBR-ENP/PPy (c, d) particles

As shown in Fig. 6 is the TEM pictures of CNBR-ENP (Fig. 6a and b) and CNBR-ENP/PPy (Fig. 6c and d) latex particles, respectively. It can be found from Fig. 6a and b that the contrast of CNBR-ENP particles is sharp, the rim of CNBR-ENP particles is clear due to the addition of small amounts of methyl acrylic acid and the surface morphology of CNBR-ENP latex particles is smooth. After the coating with PPy, CNBR-ENP/PPy particles are slightly aggregated as shown in Fig. 6c. Furthermore, it can be found from Fig. 6d that the surface morphology of CNBR-ENP/PPy particles is coarse, indicating that PPy has been deposited on CNBR-ENP latex particles. However, the resistivity of CNBR-ENP/PPy particles is beyond the upper limit of four-point probe conductivity meter (10^3 Ω·m) although the amount of PPy is as same as NBR-ENP/PPy-II particles. What is the reason? The carboxylic group on the surface of CNBR-ENP definitely has significant effect on the resistivity of this sample. In fact, PPy can be doped not only by strong acid p-TSA, but also by weak acid carboxylic acid in CNBR-ENP latex. And the resistivity of PPy doped by weak acid is higher than that doped by strong acid. Therefore, it is understandable that CNBR-ENP/PPy has higher resistivity than NBR-ENP/PPy.

The FTIR spectra of CNBR-ENP and CNBR-ENP/PPy are shown in Fig. 7. In Fig. 7a, the characteristic absorptions of CNBR-ENP particles are observed at 2925 cm^{-1} (asymmetric stretching vibration of $-CH_2$), 2853 cm^{-1} (symmetric stretching vibration of $-CH_2$), 2236 cm^{-1} (-C≡N stretching vibration), 1732 cm^{-1}, 1698 cm^{-1} (double peaks, -COO- stretching vibration), 1449 cm^{-1} (out of plane C-H wagging vibration) and 970 cm^{-1} (deformation vibration of C-H for trans $-CH_2CH=CHCH_2-$). In Fig. 8b, some characteristic peaks of PPy appear at 1558 cm^{-1}, 1291 cm^{-1}, 1036 cm^{-1} and 1051 cm^{-1}. Meanwhile, the intensities of characteristic peaks of CNBR decrease obviously. Therefore, it

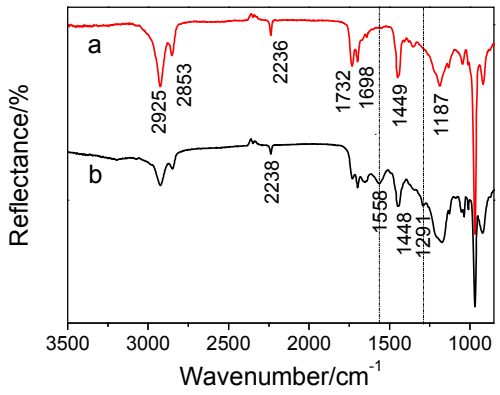

Fig. 7 The FTIR spectra of CNBR-ENP (a) and CNBR-ENP/PPy (b) particles

can be further proved that PPy have been coated on CNBR-ENP latex particles. However, in Fig. 7b, the broad absorption above 1600 cm^{-1}, arising from the free charge carriers present in the doped PPy, is much weaker than that in Fig. 3b. This phenomenon is in accordance with the result of resistivity.

3.3 Characterization of SBR-ENP/PPy latex particles

As shown in Fig. 8 is the TEM images of SBR-ENP (Fig. 8a, b) and SBR-ENP/PPy (Fig. 8c, d) particles. It can be found that not only SBR-ENP particles, but also SBR-ENP/PPy particles all aggregate seriously. In Fig. 8d, it can be found that there are many little black PPy nanoparticles with size of 15 nm to 30 nm surrounding SBR-ENP particles. The morphology of SBR-ENP/PPy particles is raspberry-like, which is different from the core-shell structure for NBR-ENP/PPy and CNBR-ENP/PPy particles. It is understandable because they used different type of emulsifiers. Both NBR-ENP and CNBR-ENP used anionic emulsions, which can adsorb pyrrole or PPy oligomers cationic radicals by electrostatic interactions; SBR-ENP is a typical nonionic latex with relatively thick hydration layer, which can inhibit the deposition of hydrophobic PPy; therefore, anionic latex particles could be coated by PPy to synthesize core-shell latex particles, while nonionic latex particles are easy to form isolated PPy nanoparticles instead. The resistivity of SBR-ENP/PPy particles is also beyond the upper limit of four-point probe conductivity meter (10^3 Ω·m) although the amount of PPy in SBR-ENP/PPy system is much higher than that in NBR-ENP/PPy system. Therefore, it is obvious that core-shell structure is more favorable for conductivity than raspberry-like structure.

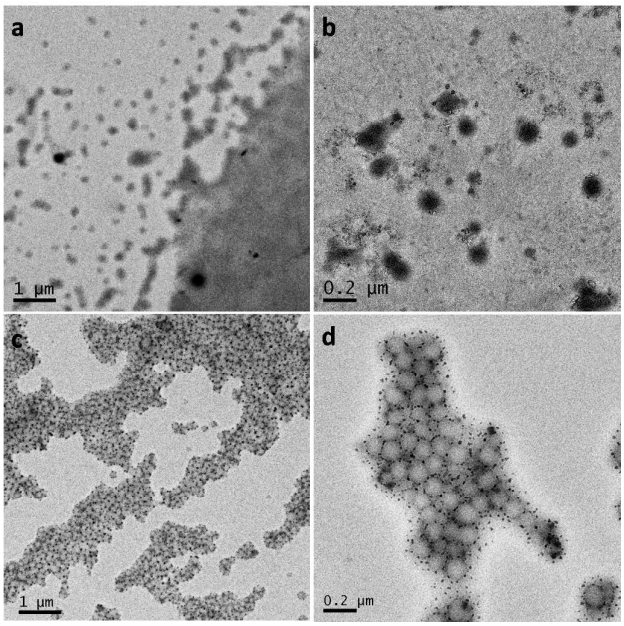

Fig. 8 The TEM images of SBR-ENP (a, b) and SBR-ENP/PPy (c, d) particles.

4. Conclusions

For the first time, an ultrafine conductive particle with core-shell structure, NBR-ENP coated with PPy, was prepared by in-situ oxidative polymerization with resistivity of 25 Ω·m. A PVA/NBR-ENP/PPy composite with resistivity of 170 Ω·m was also prepared. For comparison, the oxidative polymerization of pyrrole was carried out in CNBR-ENP and SBR-ENP latex as well. Although core-shell structure was also obtained in CNBR-ENP latex, its resistivity is much higher. Raspberry-like SBR-ENP/PPy latex particles were obtained in SBR-ENP latex with also lower conductivity than that of NBR-ENP/PPy.

References

1. A. G. MacDiarmid, *Angew. Chem. Int. Ed.*, 2001, **40**, 2581-2590.
2. J. W. Lam and B. Z. Tang, *Accounts of chemical research*, 2005, **38**, 745-754.
3. A. J. Heeger, *Synthetic Metals*, 2001, **125**, 23-42.
4. J. E. Frommer, *Accounts of chemical research*, 1986, **19**, 2-9.
5. W.-Y. Zheng, K. Levon, J. Laakso and J.-E. Osterholm, *Macromolecules*, 1994, **27**, 7754-7768.
6. F. Ghamouss, A. Brugère, A. C. Anbalagan, B. Schmaltz, E. Luais and F. Tran-Van, *Synthetic Metals*, 2013, **168**, 9-15.
7. J.-Y. Hong, S. O. Jeon, J. Jang, K. Song and S. H. Kim, *Organic Electronics*, 2013, **14**, 979-983.
8. K. Leonavicius, A. Ramanaviciene and A. Ramanavicius, *Langmuir*, 2011, **27**, 10970-10976.

9. L. Nyholm, G. Nystrom, A. Mihranyan and M. Stromme, *Adv Mater*, 2011, **23**, 3751-3769.
10. J. Pecher and S. Mecking, *Chem. Rev.*, 2010, **110**, 6260-6279.
11. M. A. Khan and S. P. Armes, *Advanced Materials*, 2000, **12**, 672-674.
12. A. Yassar, J. Roncali and F. Garnier, *polymer communications*, 1987, **28**, 103-104.
13. A. Madani, B. Nessark, R. Brayner, H. Elaissari, M. Jouini, C. Mangeney and M. M. Chehimi, *Polymer*, 2010, **51**, 2825-2835.
14. M. I. Redondo, M. V. García, E. Sánchez de la Blanca, M. Pablos, I. Carrillo, M. J. González-Tejera and E. Enciso, *Polymer*, 2010, **51**, 1728-1736.
15. Y. Lu, A. Pich, H.-J. P. Adler, G. Wang, D. Rais and S. Nešpůrek, *Polymer*, 2008, **49**, 5002-5012.
16. A. E. Wiersma, L. M. A. v. Steeg and T. J. M. Jongeling, *Synthetic Metals*, 1995, **71**, 2269-2270.
17. C. Perruchot, M. M. Chehimi, M. Delamar, S. F. Lascelles and S. P. Armes, *Langmuir*, 1996, **12**, 3245-3251.
18. S. F. Lascelles and S. P. Armes, *J. Mater. Chem.*, 1997, **7**, 1339-1347.
19. S. F. Lascelles, S. P. Armes, P. A. Zhdan, S. J. Greaves, A. M. Brown, J. F. Watts, S. R. Leadley and S. Y. Luk, *J. Mater. Chem.*, 1997, **7**, 1349-1355.
20. C. Barthet, S. P. Armes, S. F. Lascelles, S. Y. Luk and H. M. E. Stanley, *Langmuir*, 1998, **14**, 2032-2041.
21. M. A. Khan and S. P. Armes, *Langmuir*, 1999, **15**, 3469-3475.
22. M. A. Khan, S. P. Armes, C. Perruchot, H. Ouamara, M. M. Chehimi, S. J. Greaves and J. F. Watts, *Langmuir : the ACS journal of surfaces and colloids*, 2000, **16**, 4171-4179.
23. S. Fujii, S. Matsuzawa, Y. Nakamura, A. Ohtaka, T. Teratani, K. Akamatsu, T. Tsuruoka and H. Nawafune, *Langmuir*, 2010, **26**, 6230-6239.
24. J. Ormond-Prout, D. Dupin, S. P. Armes, N. J. Foster and M. J. Burchell, *Journal of Materials Chemistry*, 2009, **19**, 1433.
25. D. B. Cairns, M. A. Khan, C. Perruchot, A. Riede and S. P. Armes, *Chemistry of Materials*, 2003, **15**, 233-239.
26. S. Fujii, S. P. Armes, R. Jeans and R. Devonshire, *Chem. Mater.*, 2006, **18**, 2758-2765.
27. H. E. Cingil, J. A. Balmer, S. P. Armes and P. S. Bain, *Polymer Chemistry*, 2010, **1**, 1323.
28. D. B. Cairns, S. P. Armes and L. G. B. Bremer, *Langmuir*, 1999, **15**, 8052-8058.
29. D. B. Cairns, S. P. Armes, M. M. Chehimi, C. Perruchot and M. Delamar, *Langmuir*, 1999, **15**, 8059-8066.
30. Q. Wu, Z. Wang and G. Xue, *Advanced Functional Materials*, 2007, **17**, 1784-1789.
31. Y. Li, Z. Wang, Q. Wang, C. Wang and G. Xue, *Macromolecules*, 2010, **43**, 4468-4471.
32. J. Zhang, T. Qiu, S. Ren, H. Yuan, L. He and X. Li, *Materials Chemistry and Physics*, 2012, **134**, 1072-1078.
33. M. Y. Bai, Y. J. Cheng, S. A. Wickline and Y. Xia, *Small*, 2009, **5**, 1747-1752.
34. L. Hao, C. Zhu, C. Chen, P. Kang, Y. Hu, W. Fan and Z. Chen, *Synthetic Metals*, 2003, **139**, 391-396.
35. T. L. Kelly, S. P. Che, Y. Yamada, K. Yano and M. O. Wolf, *Langmuir*, 2008, **24**, 9809-9815.
36. F. Huang, Y. Liu, X. Zhang, G. Wei, J. Gao, Z. Song, M. Zhang and J. Qiao, *Macromol. Rapid. Commun.*, 2002, **23**, 786-790.
37. Y. Liu, X. Zhang, G. Wei, J. Gao, F. Huang, M. Zhang, M. Guo and J. Qiao, *Chinese Journal of Polymer Science*, 2002, **20**, 93-98.
38. J. Peng, J. Qiao, S. Zhang and G. Wei, *Macromolecular Materials and Engineering*, 2002, **287**, 867-870.
39. M. Zhang, Y. Liu, X. Zhang, J. Gao, F. Huang, Z. Song, G. Wei and J. Qiao, *Polymer*, 2002, **43**, 5133-5138.
40. Y. Liu, M. Zhang, X. Zhang, J. Gao, G. Wei, F. Huang, Z. Song and J. Qiao, *Macromol. Symp.*, 2003, **193**, 81-83.
41. X. Zhang, G. Wei, Y. Liu, J. Gao, Y. Zhu, Z. Song, F. Huang, M. Zhang and J. Qiao, *Macromol. Symp.*, 2003, **193**, 261-276.
42. Y. Liu, X. Zhang, J. Gao, F. Huang, B. Tan, G. Wei and J. Qiao, *Polymer*, 2004, **45**, 275-286.
43. W. Dong, Y. Liu, X. Zhang, J. Gao, F. Huang, Z. Song, B. Tan and J. Qiao, *Macromolecules*, 2005, **38**, 4551-4553.
44. G. Qi, X. Zhang, B. Li, Z. Song and J. Qiao, *Polymer Chemistry*, 2011, **2**, 1271.
45. H. Ma, G. Wei, Y. Liu, X. Zhang, J. Gao, F. Huang, B. Tan, Z. Song and J. Qiao, *Polymer*, 2005, **46**, 10568-10573.
46. Q. Wang, X. Zhang, S. Liu, H. Gui, J. Lai, Y. Liu, J. Gao, F. Huang, Z. Song, B. Tan and J. Qiao, *Polymer*, 2005, **46**, 10614-10617.
47. X. Zhang, Y. Liu, J. Gao, F. Huang, Z. Song, G. Wei and J. Qiao, *Polymer*, 2004, **45**, 6959-6965.
48. Y. Zhu, X. Zhang, Z. Song, G. Qi, X. Wang, B. Li, H. Wang and J. Qiao, *Journal of Applied Polymer Science*, 2012, **127**, 3885-3890.
49. H.-s. Wang, X.-h. Zhang, Y.-l. Zhu, Z.-h. Song and J.-l. Qiao, *Chinese Journal of Polymer Science*, 2011, **30**, 138-142.
50. H. Wang, X. Zhang, Y. Zhu, Z. Song and J. Qiao, *Materials Letters*, 2011, **65**, 2055-2058.
51. B. Li, X. Zhang, J. Gao, Z. Song, G. Qi, Y. Liu and J. Qiao, *Journal of Nanoscience and Nanotechnology*, 2010, **10**, 5864-5868.
52. Q. Wang, X. Zhang, W. Dong, H. Gui, J. Gao, J. Lai, Y. Liu, F. Huang, Z. Song and J. Qiao, *Materials Letters*, 2007, **61**, 1174-1177.
53. H. Gui, X. Zhang, Y. Liu, W. Dong, Q. Wang, J. Gao, Z. Song, J. Lai and J. Qiao, *Composites Science and Technology*, 2007, **67**, 974-980.
54. H. Gui, X. Zhang, W. Dong, Q. Wang, J. Gao, Z. Song, J. Lai, Y. Liu, F. Huang and J. Qiao, *Polymer*, 2007, **48**, 2537-2541.

55. W. Dong, X. Zhang, Y. Liu, Q. Wang, H. Gui, J. Gao, Z. Song, J. Lai, F. Huang and J. Qiao, *Polymer*, 2006, **47**, 6874-6879.

56. W. Dong, X. Zhang, Y. Liu, H. Gui, Q. Wang, J. Gao, Z. Song, J. Lai, F. Huang and J. Qiao, *European Polymer Journal*, 2006, **42**, 2515-2522.

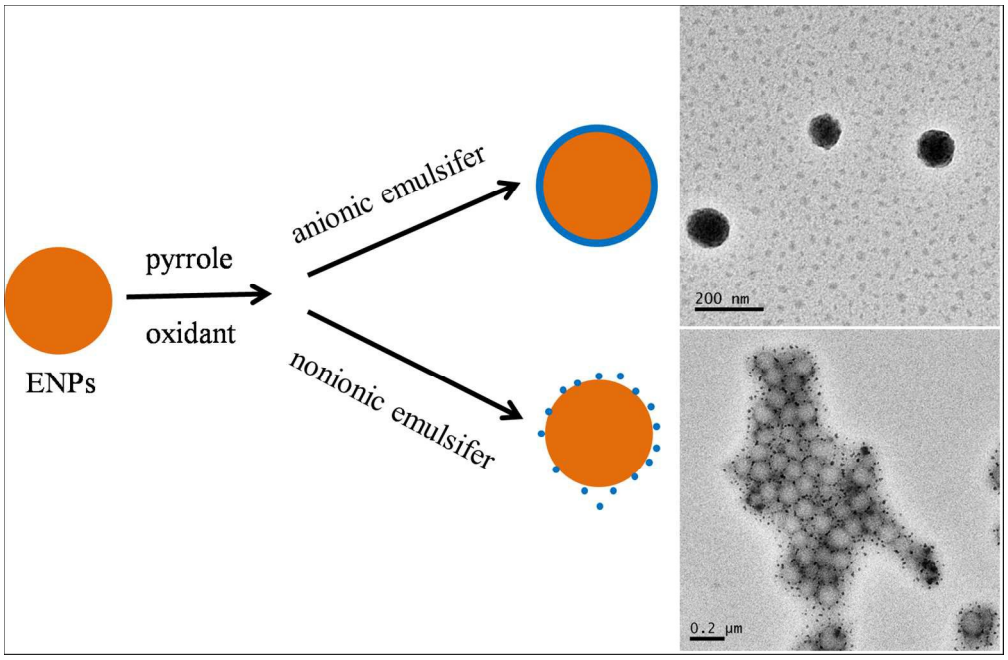

Graphical abstract
276x178mm (150 x 150 DPI)